Technical Paper

Hardening, microstructure, and shrinkage development of UHPC: A review

Jianhui Liu, Caijun Shi[*], and Zemei Wu

Abstract: Ultra-high performance concrete (UHPC) refers to cement-based materials exhibiting compressive strength higher than 120 MPa, high ductility, and excellent durability. High cracking tendency of UHPC derived from autogenous shrinkage can be a concern due to its high binder content and low water to binder ratio (w/b). This paper reviewed early hardening, microstructure, and shrinkage development of UHPC. The effect of supplementary cementitious materials (SCMs), such as silica fume (SF), ground granulated blast-furnace slag (GGBS), fly ash, limestone powder, rice husk ash, and nano-materials, and curing methods on hydration and microstructure was reviewed. In addition, the effect of cement, water content, aggregate, chemical admixtures, SCMs, curing methods, and fiber on the shrinkage of UHPC was summarized. Different methods to compensate and/or reduce the early-age shrinkage of UHPC were introduced.

Keywords: Ultra-high performance concrete (UHPC); hydration; microstructure; autogenous shrinkage.

1. Introduction

Ultra-high performance concrete (UHPC) refers to cement-based materials with excellent mechanical properties [1-3]. With the incorporation of steel fiber, the ductility and energy absorption of UHPC are typically 300 times greater than that of high performance concrete (HPC) [3]. UHPC possesses excellent durability [4], which is nearly impermeable to carbon dioxide, chlorine ion and sulphates. Its superior durability can increase service life and reduce maintenance [5]. The enhanced abrasion resistance of UHPC provides extended life for structural elements, such as bridge decks and industrial floors. At the same time, it can also provide protection to areas under corrosive or harsh climate conditions [6]. Due to ultra-high compressive strength, UHPC structures weigh only one-third or one-half of conventional concrete structures under the same load [3]. This allows production of more slender structures, which increases usable floor space in high-rise buildings and reduces overall costs. Elimination of
steel reinforcement reduces labor costs and provide greater architectural space, allowing nearly limitless structural member shapes and forms for architects and designers [6].

Though UHPC possesses many outstanding properties, the low water-to-binder ratio (w/b) in UHPC and use of high content of fine supplementary cementitious materials (SCMs), such as silica fume, can lead to self-desiccation and even cracking in some cases [7]. Autogenous shrinkage is one of the most important issues that needs to be considered for UHPC, especially at early stage [8]. High autogenous shrinkage was found during the first one or two days after mixing due to the initial hydration, which can cause a considerable cracking potential at early ages. Different research with different mix proportions would result in different shrinkage [9-13]. Autogenous shrinkage up to 1000 με at 28d was reported by Liu [14]. The difference in shrinkage values was related to the water-to-cement ratio (w/c) or water-to-binder ratio (w/b), cement type, types and amounts of SCMs, use of aggregate, curing methods, and fiber characteristics. Therefore, it is very importance to clarify the factors influencing autogenous shrinkage of UHPC.

Large shrinkage, especially the autogenous shrinkage, is one of the main characteristics of UHPC, which may induce cracking in the UHPC structures, therefore it is very important to control the shrinkage of UHPC. In addition, the development of shrinkage

Jianhui Liu is a Researcher at the College of Civil Engineering, Hunan University, China.
Corresponding author Caijun Shi is a Professor of the College of Civil Engineering, Hunan University, China.
Zemei Wu is a Researcher at Hunan University, China.

in UHPC is related to the hydration and microstructure of UHPC. Therefore, this paper reviewed hardening, microstructure, and shrinkage development of UHPC in order to provide some insights and suggestions for further research, and to facilitate the applications of UHPC. Factors including cement and water content, aggregate, chemical admixtures, pozzolanic materials, curing conditions, and fiber, were discussed. Some preventive measures for reducing autogenous shrinkage were discussed in order to mitigate shrinkage and improve the cracking resistance of UHPC.

2. Hardening of UHPC

2.1 Hydration process of UHPC

The addition of SCMs has an important influence on hydration of UHPC. UHPC usually contains 10-30% silica fume (SF) based on the mass of total binder materials. It is well known that silica fume could accelerate the hydration of cement in conventional concrete. It also has great influence on the hydration of binder material in UHPC [15] (Fig. 1). As can be seen from Fig. 1(a), compared to the reference mixture U0 (without silica fume, w/c=0.18), the use of silica fume decreases the dur-ation of dormant period of UHPC matrix from 12h to 9h or less. As hydration proceeds, UHPC mixtures with 25% silica fume (U25) shows the accelerated hydration peak first, followed by those of U20, U15, and U10, with 20%, 15%, and 10% silica fume, repectively. However, the hydration peak of U0 is delayed to 28h. The heat of hydration of UHPC mixture with silica fume evolves faster than that of the reference sample [15]. This is due to the fact that the incorporation of silica fume can absorb Ca^{2+} and OH^- ions to form calcium silicate hydrate (C-S-H), which increases the rate and amount of heat evolution [16]. However, when the silica fume content increased to 30%, the heat evolution rate decreased and the accelerated hydration period increased [17]. Partial replacement of cement with ground granulated blast-furnace slag (GGBS) or fly ash can retard hydration mainly during the dormant and acceleration periods [17, 18], as shown in Fig. 1(b). However, the combined use of silica fume and fly ash is significantly different from the hydration of pure cement at w/b of 0.35 [19]. This may be due to the reason that silica fume particles dominate the hydration at very low w/b. There is also a slight retardation tendency for the hydration heat of the mixtures with silica fume and GGBS [17]. Limestone powder (LP) can accelerate the hydration of cement [20, 21] and improve the hydration degree of binder materials [22-25]. Use of rice husk ash (RHA) also increases the degree of hydration of cement at later ages because of the pozzolanic rea-

tion and internal curing, even higher than those containing silica fume at 91d [26, 27].
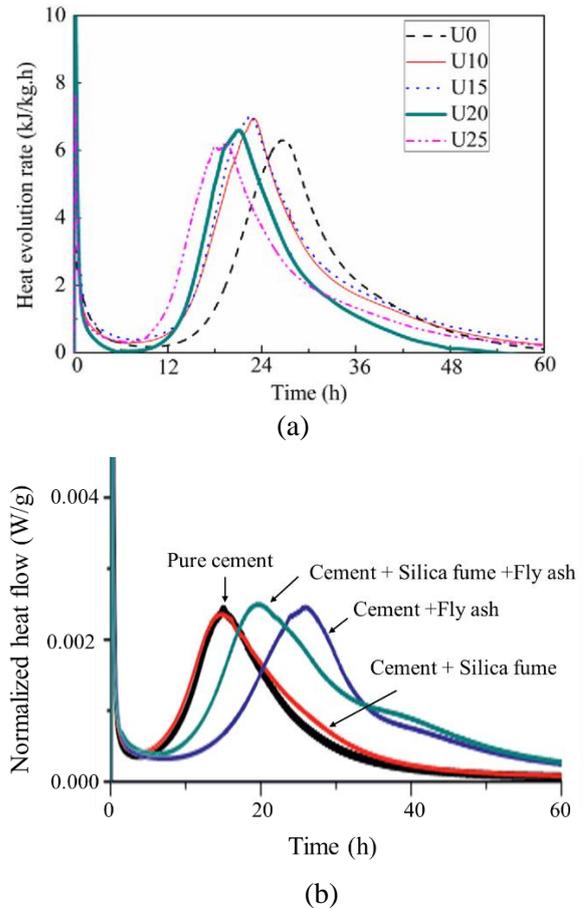

(a)

(b)

Fig. 1 Heat evolution rate of UHPCs: (a) with different silica fume contents (U0, U10, U15, U20, and U25 represent use of 0%, 10%, 15%, 20%, and 25% silica fume by the total mass of binder materials, respectively) [15]; (b) with different contents of silica fume and fly ash [18].

It is well known that nanomaterials can provide significant enhancement in performance of cement-based material given their physical (filling and nucleation) effects as well as the chemical reactivity. The addition of nanomaterials not only shortened the dormant period but also led to an earlier appearance of the acceleration periods, which have been reported by some references [28, 29]. According to reference [11], the dormant period of the reference mixture is around 13h, the addition of nano-$CaCO_3$ shortens the dormant period to about 9h due to the filling and chemical effects induced by nano-$CaCO_3$ [30]. However, the addition of 4.8% nano-$CaCO_3$, by mass of binder materials, causes an earlier and higher heat of hydration than the addition of 6.4% nano-$CaCO_3$. This might be due to a dilution effect associated with the addition of nano-$CaCO_3$ when it is used as a substitution of cement. Nano-SiO_2 can also accelerate the heat of hydration due to its filling effect and nucleation seed for the precipitation of C-S-H

[31]. Meng and Khayat [32] found that both of carbon nanofiber (CNF) and graphene nanoplatelet (GNP) increased the cumulative hydration heat when CNF reduced induction period, and the use of nano-platelet extended the induction period. It is attributed by the fact that the dispersion of CNF needs less super-plasticizer than GNP, and this behavior is also found in the use of aluminum oxide nanofibers [33]. On the other hand, Norhasri [34] reported that the addition of nano metaclay had a retarding effect on UHPC due to increase of surface area from the nano metaclay.

On the other hand, due to the high dosage poly-carboxylate superplasticizer (2%-4%, by mass of binder materials) in UHPC, the early hydration of binder in UHPC is usually retarded. The retardation is dependent on the type and dosage of the super-plasticizer. In addition, the increase of curing temp-erature can accelerate the hydration of cement and promote the secondary hydration between SCMs and $Ca(OH)_2$ [35], which has a great influence on the hydration products (See the next section).

2.2 Hydration products

The hydration products of binder materials in UHPC is similar to those in ordinary concrete (OC). In UHPC, it contains a larger amount of SCMs. Initi-ally, Portland cement hydrates to form calcium sili-cate hydrate (C–S–H) and calcium hydroxide (CH). Then, SCMs, such as silica fume, GGBS, and fly ash reacts with CH to form C–S–H [36]. The amount of CH is much lower than that in OC at 28 days as shown in Fig. 2, but the pozzolanic reactions are still incomplete. Different SCMs have different influ-ences on CH content of UHPC. When the silica fume content increases from 0 to 50%, the calcium hy-droxide content decreases from 7.4% to 6.25% [17]. Both RHA and SF can strongly reduce CH content, and the effect of SF is greater than that of RHA at later ages [26]. However, the effect of GGBS content has limited effect on the CH content [17]. Shi and Wang [17] found that the combination of silica fume and GGBS had negative synergistic effect on the cal-cium hydroxide content of UHSC, but no explana-tion was given.

The content of crystalline phases is considera-bly higher in OC, whereas less amorphous phases were observed in the UHPC as shown in Fig. 2 [36]. Because of no considerable phase carbonation in UHPC, no calcite is measured even after 28 days in this specimen. The variations of ettringite content development between the first day and the second day indicate some conversion of ettringite to mono-sulfate phase, and that significant amount of alumi-nate may enter the X-ray amorphous C–S–H phases [36]. When UHPC contains LP constituents, calcium aluminate monocarbonate is preferably formed, the

hydration of C_3S is accelerated, and some carbo-silicates are produced in the pastes [37]. Other liter-atures [38, 39] shows that LP in binder materials systems has a compaction filler and great dispersion effect on the precipitation of $Ca(OH)_2$ and C–S–H gel, and plays a core role in crystallization during the hydration of cement.
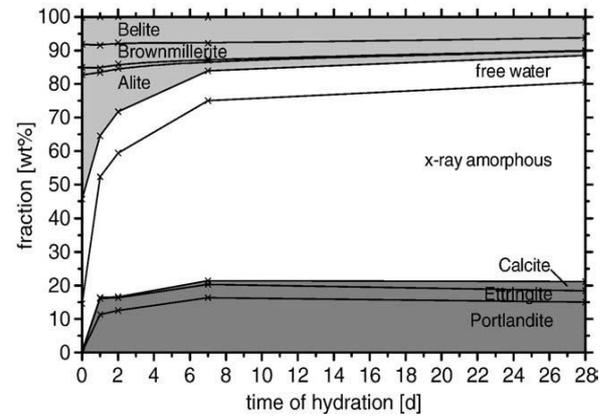
(a) Ordinary concrete (OC)
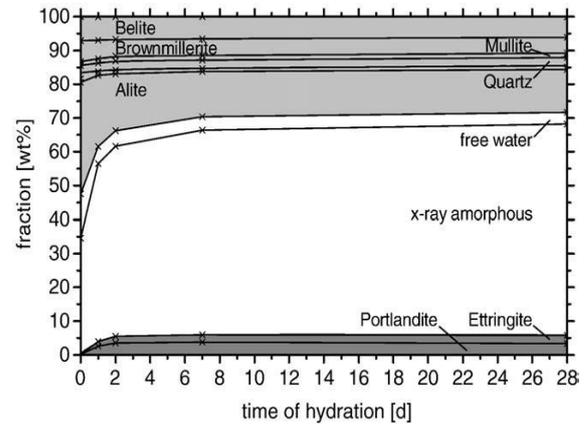
(b) Ultra-high perfomance concrete (UHPC)

Fig. 2 Time-dependent phase development in OC and UHPC [36]

The increase of curing temperature can acce-lerate the hydration of cement and promote the pozz-olanic reaction between SCMs and CH [35]. Hydra-tion products of cement after curing at 90 °C remain amorphous. On the condition of no external SiO_2 source, the hydration of C_3S and C_2S leads to form-ation of crystalline α-dicalcium silicatehydrate. On the other hand, tricalcium aluminate (C_3A) and tetr-acalcium alumino-ferrite (C_4AF) form a hydrogarnet phase. The bonding properties of these two phases are rather unfavorable. If finely ground quartz and/or other SiO_2 sources are used, a pozzolanic reaction takes place between CH and SiO_2, yielding crys-talline 1.1 nm tobermorite ($C_5S_6H_5$) as the main pro-duct of reaction at temperatures between about 150 °C and 200 °C. Xonotlite C–S–H (I), C–S–H (II), and a-C_2SH may also be formed at even higher temperature [40]. The formation of both 1.1 nm tobe-

rmorite and xonotlite can increase strength of auto-claved products [41]. It is clear from Fig. 3 and Table 1 [42, 43] that there is an important effect of temperature on hydration of UHPC. Hydrates formation ratio increases from 10% to 55% when the cur-ing temperature increases from 90°C to 250°C. It is also significant to notice that Q2 increases faster with temperature higher than Q1 (Fig. 3). This indicates that C-S-H average statistical chain length increases with temperature. This point is also clearly demon-strated by statistical average chain length that corre-sponds to pentamer at 200°C when it is trimer at 90°C or 200°C. Between 200 and 250°C, another microstructural change is observed with the appea-rance of a Q3 peak at 250°C (Fig. 3). This peak is attributed to the presence of a crystal hydrate, xono-tlite, whose structure implies the presence of silicon-oxygen tetrahedra connected to three neighbor tetra-hedra (Q3 species). The H/C (H_2O to CaO) ratio of C–S–H of OC is approximately one, while the H/C of xonotlite is 1/6, and xonotlite forms only in the inner part of concrete specimen [44]. The formation of xonotlite in heat-cured UHPC is due to local, large water vapor pressures. However, lower dynamic eq-uilibrium vapor pressures (3 Pa) can totally suppress the formation of crystalline hydration products, and even no xonotlite or other crystalline hydration prod-ucts forms at 250°C [45].

3. Microstructure development

UHPC has a very dense and uniform micro-structure according to following fundamental effects: (1) close packing of solid particles; (2) hydration and pozzolanic reactions of binder; (3) improvement of the interfacial transition zone (ITZ) between aggre-gates and bulk matrix [2]. The internal microstru-cture of UHPC mainly includes unhydrated cement particles, quartz sand, and hydration products, such as C–S–H [46]. The microstructure of UHPC depe-nds on the pore structure, morphology of hydration products, and microstructure of ITZ.
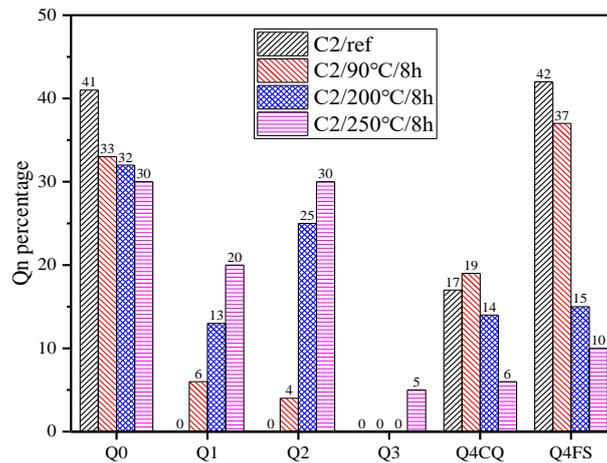

Fig. 3 Percentages of Q0 to Q4 for specimens with heat treatment at 90, 200, and 250°C for 8h [43].
NOTE: Q represents a SiO_4^{4-} unit and the degree of connectivity, n is related to the oxygen bonds number between the SiO_4^{4-} units (Q4FS for silica fume and Q4CQ for crushed quartz)

Table 1 Hydrates formation ratio H, connectivity ratio C, average statistical chain length, pozzolanic activity of silica fume PSF and crushed quartz PCQ of samples with heat treatment at 90, 200, and 250°C [43]

Samper	H	PSF	PCQ	C	Statistical length
C2/REF	0%	0%	0%	-	-
C2/90°C/8h	10%	10%	0%	1.40	Trimer or quadrimer
C2/200°C/8h	40%	65%	20%	1.65	Pentamer or hexamer
C2/250°C/8h	50%	75%	65%	1.73	Hexamer or heptamer

NOTE: Hydrates formation ratio H=(Q1 + Q2 + Q3); connectivity ratio C= (Q1 + 2Q2 + 3Q3)/(Q1 + Q2 + Q3); poz-zolanic activity of silica fume PSF=(Q4FS-Q4FS$_0$)/Q4FS$_0$; crushed quartz PCQ = (QCQ4 – QCQ4$_0$)/QCQ4$_0$.

3.1 Pore Structure

UHPC is designed by close packing density and use of SCMs. Therefore, it has a very low porosity. For UHPC at water to binder ratio (w/b) of 0.20, its capillary pores become discontinuous when only 26% of cement is hydrated, instead of 54% for HPC (w/c = 0.33) [47]. Figure 4 shows the pore radius distribution, measured using high-pressure mercury intrusion porosimetry, of a high-quality class C45/55 normal-strength concrete, a class C90/105 high-strength concrete, and two UHPC mixes (90°C heat treatment, coarse- and fine-grained mixes) [48]. The porosity of UHPC consists mainly of pores with diameter smaller than a threshold value (Fig. 5), and a reduction of cumulative porosity corresponds with a decrease in the threshold value. The pore size of UHPC basically concentrates between 2 and 3 nm, the most probable pore diameter is 2.0 nm, and its total porosity is 2.23%.

The curing method and temperature have great influence on pore structure of UHPC. It is nil in the range of 3.75 to 100 nm for UHPC cured at between 150 and 200°C [44]. When the curing temperature is from 20°C to 65°C, setting pressure had no influence on the cumulative porosity in the range of 3.75 nm to100 μm. However, setting pressure is able to eliminate the air trapped in sample and to compact the sample. A portion of free water is also eliminated. In that range of temperature, the porosity threshold is not modified. For curing temperatures between 80 and 200°C, lower cumulative porosity, intermediate (3.75 nm to 100 μm) porosity and threshold pore size is obtained for pressed samples. The greater part (B 90°C/SC, Fig. 5) if not the whole porosity (BQ 200°C/P, Fig. 5) corresponds in that case to pore diameters smaller than 3.75 nm. For temperatures of 250°C and above, the porosity increases, as well as the threshold pore size (see BQ200°C/P and BQF400°C/SC in Fig. 5).
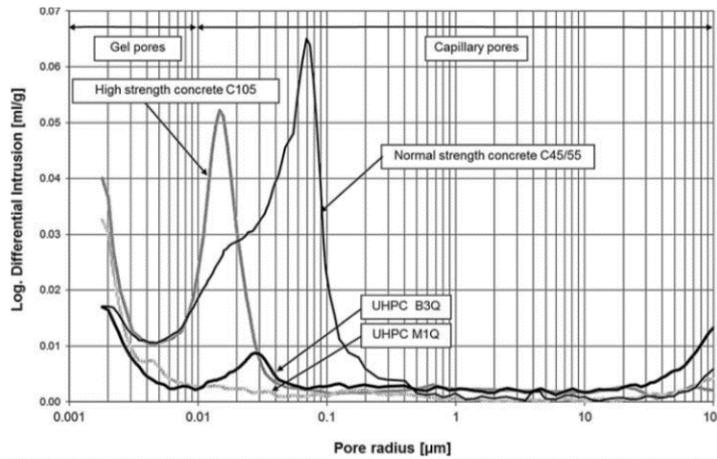

Fig. 4 The pore radius distribution of normal-strength concrete, high-strength concrete and two UHPC mixes
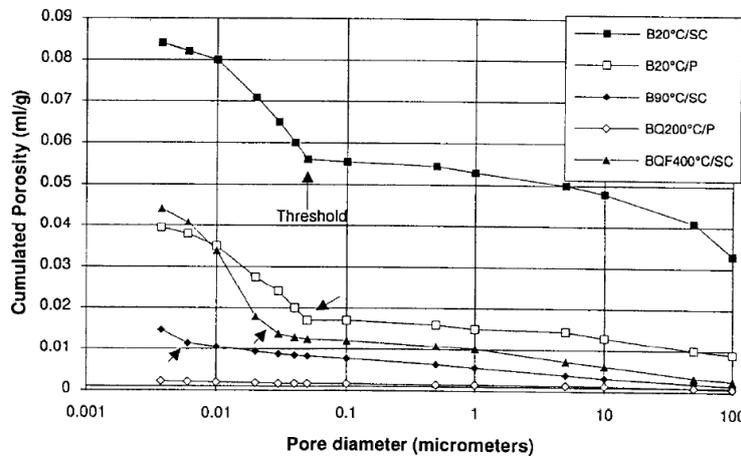(90°C heat treatment, coarse- and fine-grained mixes) [48]

Fig. 5 Cumulative porosity versus pore diameter of UHPC [44]

NOTE: B20°C/SC, Basic formulation heated at 20°C, soft cast (setting pressure, 1 atm); B20°C/P, Basic formulation heated at 20°C, pressed (setting pressure, 30 atm); B90°C/SC, Basic formulation heated at 90°C, soft cast; BQ200°C/P, Basic formulation with crushed quartz heated at 200°C, pressed (setting pressure 625 atm); BQF400°C/SC, Basic formulation with crushed quartz and steel fibers heated at 400°C, soft cast

The porosity of UHPC decreases with the increase of silica fume content due to its filling and pozzolanic effects [17]. When silica fume content increases from 0% to 50%, the 3d porosity decreases from 14% to 12.7%, and the 56d porosity decreases from 10.4% to 8.3%. If the silica fume content is higher than 25% and GGBS content is less than 25%, GGBS has little effect on the porosity of UHPC at 3d. However, GGBS at any content would increase the porosity of UHPC at 56d. The combination of silica fume and GGBS can cause a negative synergistic effect on the porosity of UHPC in reference [17], but no explanation was given. The total porosity of the RHA modified is higher than that of the SF modified sample, but lower than that of the control sample because of greater filler effect and pozzolanic reaction [26]. The use of 0.3% carbon nanofiber (CNF) can reduce the total porosity of the UHPC by approximately 35%, indicating that the presence of CNF can refine the microstructure of UHPC [32].

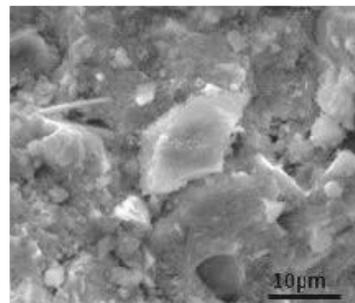### 3.2 Morphology of hydration products

UHPC is composed of aggregates and compact matrix phase, including unhydrated particles, quartz sand, and hydration products. A reactive interface is formed between completely unhydrated core and hydration products. The core plays a role in skeleton to matrix, and greatly enhances the microstructure of matrix phase [49]. Scanning electron microscope (SEM) observation indicates that the structure of hardened paste is very dense due to very low w/b,

hydration of cement, and the pozzolanic action of SF and GGBS. The main hydration product C–S–H gel is homogeneous, no $Ca(OH)_2$ and ettringite could be found [20, 50]. The curing method has a great influence on microstructure of UHPC, as shown in Figs. 6 and 7.

Fig. 6 shows the microstructures of UHPC samples under different curing conditions. From Fig 6(b), it can be observed that there is clear unhydrated binder constituents in UHPC, which are adhered to several hexagonal CH crystals before heat curing, thus leading to relatively loose microstructure compared to UHPC after heat curing. Visible microcracks are also found propagating along the boundaries of the CH crystals in Fig. 6(b). However, the microstructures of the UHPC samples after10h of heat curing become much denser compared to that before heat curing, as shown in Fig. 6(c). At the same time, it is less likely to observe the CH crystals in the sample after heat curing. Similarly, in Fig. 6(d), the even denser microstructure of sample after 48h of heat curing confirms that the chemical hydration degree is further higher. The reason is that during heat curing, the high-density nano-crystalline layers typically forms calcium was distinctly difficult to detect the extreme-value of the pore distribution curve. This indicates that heat curing can effectively accelerate chemical hydration of UHPC and form more hydrated products to fill up the pores and voids of the internal structure, resulting in denser microstructure and small pores [51].
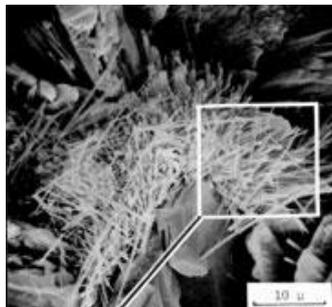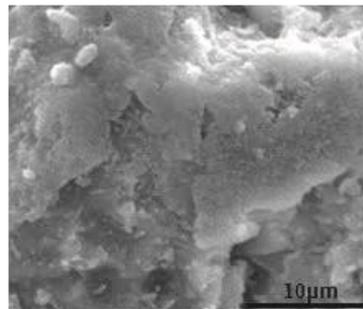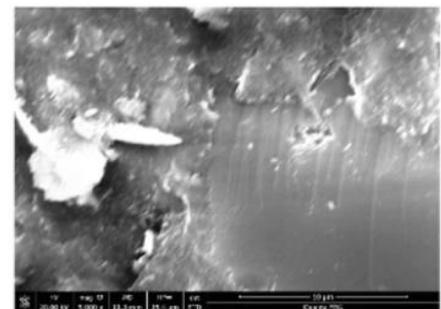

(a) Cement matrix in conventional concrete [52]   (b) UHPC under room curing [53]
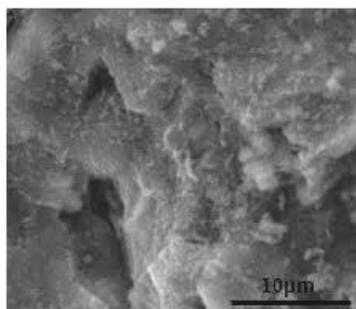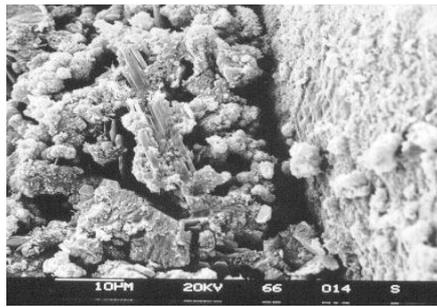

(c) UHPC after 10h of steam curing [53]
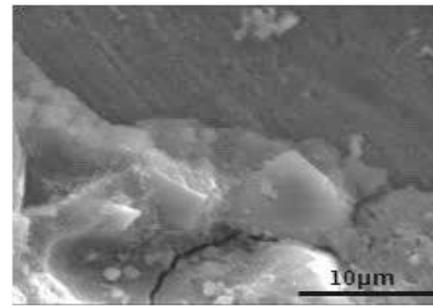
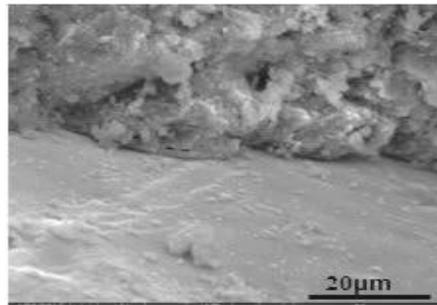(d) UHPC after 48h of steam curing [53]

(e) UHPC after autoclave curing [35]

Fig. 6 Microstructure of conventional concrete and UHPC under difdferent curing conditions
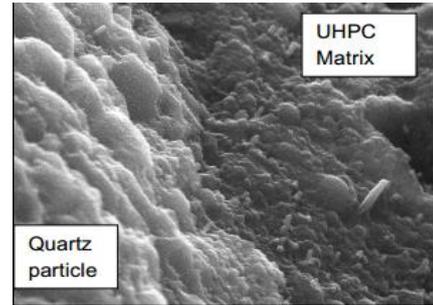
(a) ITZ in conventional mortar [2]

(b) UHPC under room curing [53]

(c) UHPC after 48h of steam curing [53]

(d) UHPC after autoclave curing [58]

Fig. 7 ITZ of conventional mortar and UHPC under different curing conditions
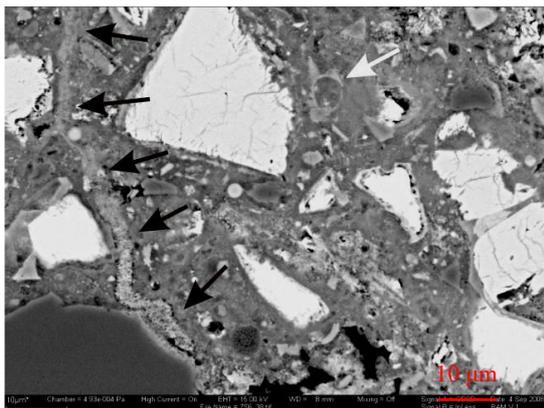

Fig. 8 SEM image of autoclaved UHPC specimen at 200°C/15 bars. A crack is filled with crystalline C-S-H (black arrows). The white arrow points to a completely hydrated grain of fly ash, which indicates a high degree of pozzolanic reaction [57]
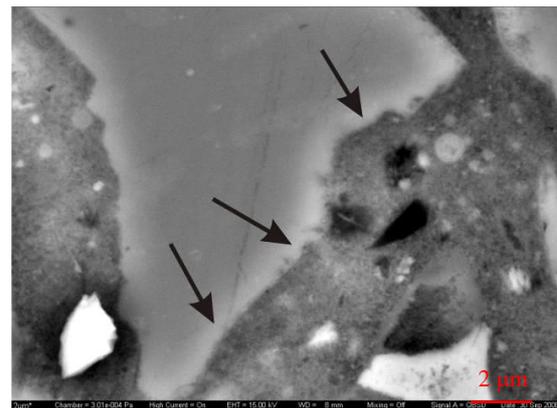

Fig. 9 SEM image of autoclaved UHPC specimens at 200°C/15 bars. Dissolution rims on a grain of the quartz filler producing strong cohesion with crystalline cement paste (black arrows) [57]

3.3 Microstructure of ITZ

The microstructure of interfacial transitional zone (ITZ) in conventional cement mortars and UHPC from SEM observations are shown in Fig. 7. It can be seen that the ITZ between aggregates and paste matrix has a high porosity and CH content, and is the weakest part in conventional concrete. However, UHPC has a very dense ITZ without obvious pores [20]. Normally, the microstructure of the ITZ is influenced by the "wall effect" in the vicinity of aggregate surfaces. This region is about 50 μm from the grain surface into the cement paste [54]. However, in reference [26], sand with particle sizes ranging from only 100 to 300 μm is used as the main aggregate. This can reduce the "wall effect" and thickness of the ITZ. Moreover, with such a small sand particle size and a very small thickness of the ITZ, the effect of SCMs, such as SF or RHA, in reducing the ITZ thickness could not be significant. Therefore, the thickness of the ITZ of all samples obtained in this study is similar and very small. However, owing to the low w/b and pozzolanic reactions between CH and reactive mineral admixture, which consumes most of the CH crystals and converts them to C–S–H [1, 55], the ITZ in UHPC seems as dense as the matrix. The homogenous structure is important for the excellent performance of UHPC.

The denser microstructure of ITZ in UHPC is closely related to high temperature curing. When UHPC is cured in the hot water at 90°C for 10h, the hydration products become denser, and basically the existence of calcium hydroxide cannot be seen (Fig. 6(c)). Increased curing temperature could accelerate the hydration reaction of cement and pozzolanic activity, and improve the microstructure of ITZ [44]. Autoclave curing can improve degree of hydration, and a homogeneous, dense microstructure consisting of close networked crystal fibers with length up to one micrometer would occur under the autoclave curing condtion. Cracks and small pores are filled with crystalline C-S-H, as shown in Fig. 8. The pore volume was lower than the heat treated specimen and the median pore diameter was reduced to 5 nm when autoclace curing was used. The autoclaved specimens exhibits dissolution processes around quartz grains, which produces a better cohesion between fillers and fine crystalline cement paste (Fig. 9) [56, 57]. In addtion, the heat curing and autocalve curing can also improve the microstrcture around the steel fiber [35].

4. Autogenous shrinkage of UHPC

4.1 Factors affecting autogenous shrinkage of UHPC

4.1.1 Binder and water contents

Shrinkage of concrete is usually caused by loss of water due to evaporation or by chemical change resulted from the hydration of cement. Concrete with higher w/b has higher drying shrinkage but lower autogenous shrinkage. For UHPC, the w/b normally is less than 0.25, and the autogenous shrinkage accounts for up to 80% [14]. In addition, the increase in cement content and the decrease in water amount would cause a greater autogenous shrinkage [59]. A higher rate of hydration results in higher autogenous shrinkage due to the decreased volume of hydration products relative to their constituents and higher water consumption. These could reduce bleeding and increase the concrete temperature [60, 61]. It has a major role on early-age shrinkage through controlling the amount of free water, and the development of the microstructure and pore system, which consequently affects the capillary tension and meniscus development (autogenous shrinkage). The strains of samples with lower w/c are higher than those with higher w/c, as shown in Fig. 10. Moreover, cement containing more C_3A content (cement B) led to higher strains. In addition, the shrinkage increases with w/c, when the UHPC is made by cement B (8.6 % C_3A content by mass). This confirms the importance of the C_3A for the autogenous shrinkage of UHPC [9].

4.1.2 Aggregate

Aggregates can act as an internal restraint to reduce shrinkage. It can also reduce the volume of cement paste, leading to lower chemical shrinkage [60]. For UHPC, Meng et al. found that the auto-genous shrinkage is reduced with increase of sand to binder ratio [59]. However, Xie et al. [62] reported that the autogenous shrinkage increased with increase of sand to binder ratio. Different con-clusions for these two references may be attributed by the fact that the two research results choose different test zeros time for autogenous shrinkage. In addition, the particle size and clay content of aggregate have a significant influence on shrinkage of UHPC. Ma et al. [47] reported that the autogenous shrinkage could be considerably reduced by incorporating basalt coarse aggregates with size ranging from 2 to 5 mm. In addition, there was no swelling in the UHPC specimens produced with coarse aggregates after initial shrinkage, while swelling was observed in UHPC without coarse aggregates [63]. It was found that the shrinkage strain rate linearly increased with clay content of fine aggregate [64]. Furthermore, light-weight aggregates (LWAs) with high water absorption were found to reduce autogenous shrinkage as they act as internal curing materials [8, 65-67]. The shrinkage-reducing efficiency in UHPC is related to the particle size [66], content [65, 67], water absorption [68] and pretreatment method [65] of LWA. For UHPC, it is recommended that use of 15-25% fine LWA is optimal content [67, 69].

### 4.1.3 Supplementary cementitious materials (SCMs)

The type, fineness, and percentage of SCMs have very significant effect on autogenous shrinkage of UHPC. Silica fume was found to significantly increase the autogenous shrinkage due to refinement of pore structure [70, 71]. Similar increased autogenous shrinkage was observed for GGBS [72, 73]. A high level of cement replacement by metakaolin (10%-15%) was found to reduce both the autogenous and drying shrinkage at early-ages, as shown in Fig. 11(a) [74]. This reduction may be a result of the dilution effect of reducing the cement content [75, 76]. Staquet et al. [77] found that use of metakaolin to substitute 2/3 SF would cause a reduction of around 50% in autogenous shrinkage of UHPC at 6d. In addition, the curing temperature had some influences on the shrinkage reducing effects of metakaolin. Significant reduction of early age autogenous shrinkage was obtained by replacing silica fume with metakaolin in specimens cured at 20°C [48]. However, for UHPC cured at 42°C, the total shrinkage measured for a mixture containing metakaolin was negligible compared to those with silica fume or fly ash [49]. However, Song et al. [28] suggested that the combination

of 60% SF with 40% MK significantly decreased the pore size distribution of UHPC into the range of about 5–10 nm compared to the UHPC with 0% and 100% MK, and it may cause a high autogenous shrinkage. However, there is no autogenous shrinkage results in this reference. Incorporation of fly ash could decrease the shrinkage of concrete, because the unhydrated binder material acted as aggregate to restrain shrinkage and it also diluted cement content [78, 79]. In contrast, it was reported that very fine fly ash had a similar effect to that of silica fume [70]. RHA markedly decreased the autogenous shrinkage due to its internal curing effects on restraining the drops of internal relative humidity [80-82], as shown in Fig. 11(b).
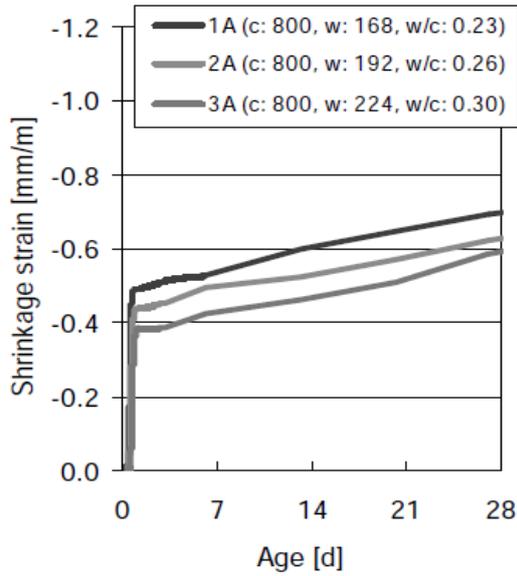
(a) variation of w/c at constant content
(cement A)
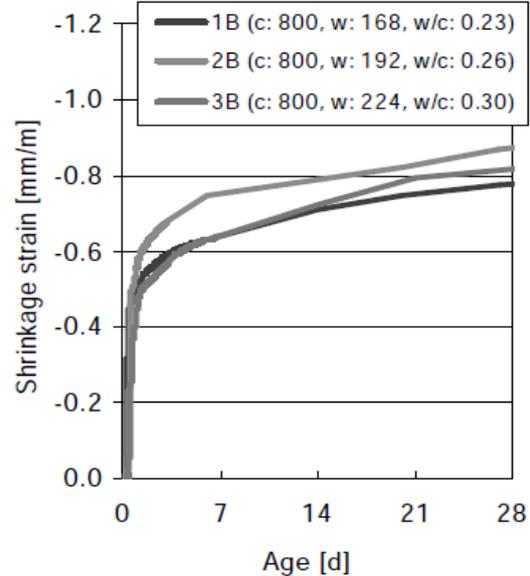
(b) variation of w/c at constant content
(cement B)
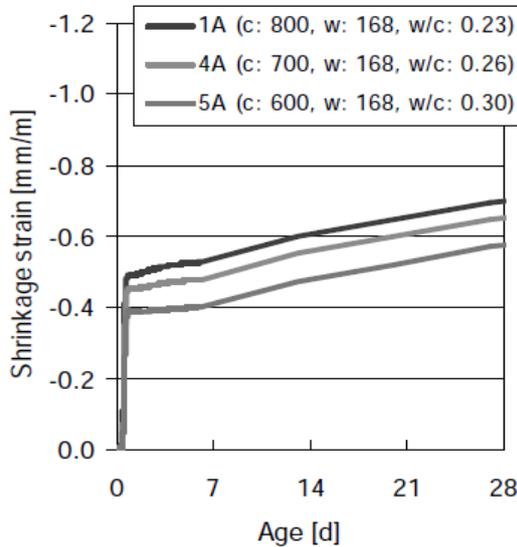
(c) variation of w/c at constant water content
(cement A)

(d) variation of w/c at constant water content
(cement A)

Fig. 10 Autogenous shrinkage vs. age: variation of w/c at constant cement content and variation of cement content at constant water content [9].

NOTE: Cement B contained considerably more C3A (A: 2.0 mass %; B: 8.6 mass %); 16.2% silica fume by mass.

(a) Metakaolin [74]

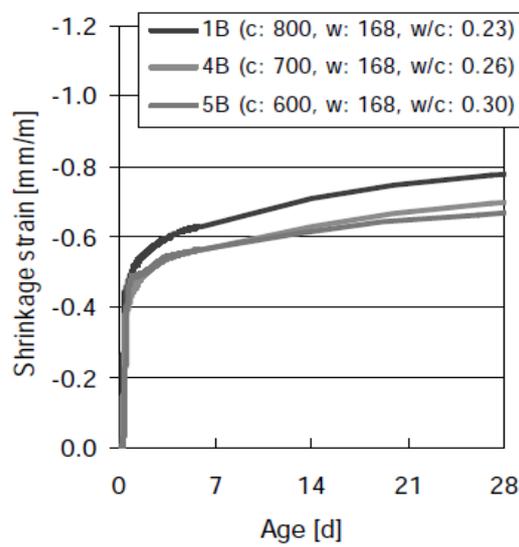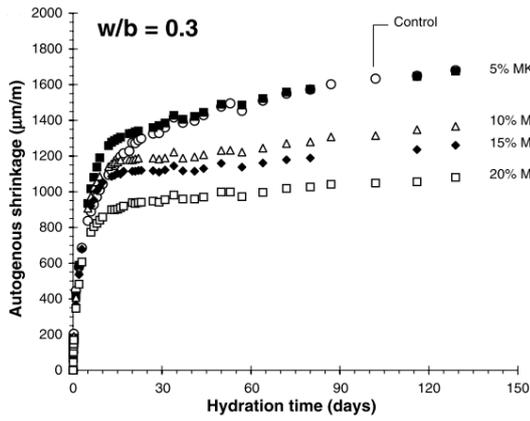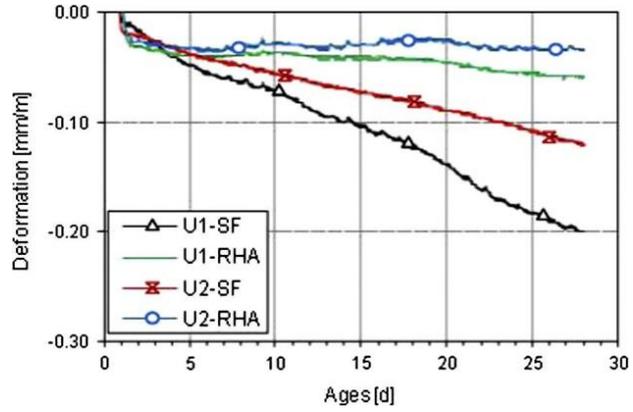(b) SF and RHA [83]

Fig. 11 Effects of pozzolanic materials on autogenous shrinkage

4.1.4 Chemical admixtures

Greater early-age shrinkage of cement and mortar was observed with the addition of superplasticizer (SP) as a result of improving cement dispersion, which consequently increased the rate of hydration [60, 61]. However, Eppers [9] showed that the superplasticizer content had no influence on the shrinkage of UHPC at the age of 28d, although it had a significant effect on the early age behavior. Shrinkage reducing admixtures (SRAs) belong to a class of organic chemicals known as surfactants [84-87]. SRA can decrease the surface tension of the capillary pore solution resulting in a reduction of the capillary tension and led to a significant reduction in autogenous shrinkage of UHPC [88]. Furthermore, SRA lowered the evaporation rate in the matrix and delayed the mass loss in the drying conditions [85, 89]; and hence the drying shrinkage was reduced. Expansive agent (EA) is categorized as iron powder, alumina powder, magnesia, calcium sulfoaluminate, and calcium oxide. Suzuki et al. [90] reported that an autogenous shrinkage of more than 700 millionths would be reduced to zero with the use of EA. However, the expansion action of EA increased water demand. A combination of EA and internal curing exhibits high efficacy in mitigating shrinkage [91], because internal curing could provide more water for concrete. Recently, a new type of internal curing materials, superabsorbent polymer (SAP) was used for reducing shrinkage of UHPC [8, 14, 89], as shown in Fig. 12. SAP has water absorption capacity of up to 1000 times of their own mass [92] and its internal curing function is based on the release of water from saturated SAP into the matrix as the relative humidity drops over time. The effectiveness of SAPs is related to its chemical characteristics [93-95], dosage [8, 96], particle size [97, 98], and w/b of the matrix [99-101].
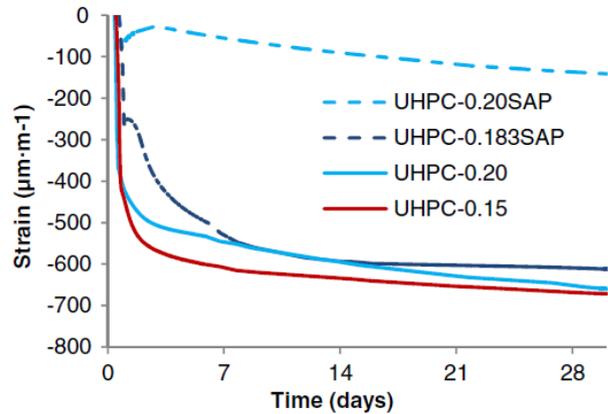
Fig. 12 Autogenous deformation of UHPC with different w/c ratios and SAP additions in the first 30 days of hydration. The results were zeroed at the final setting time of the corresponding cement pastes. Each curve is the average of triplicate samples [102]

4.1.5 Curing condition

Curing method, duration, and temperature have a significant effect on autogenous shrinkage of UHPC. Normally, an early-age drying environment would cause a higher shrinkage for normal concrete and high-performance concrete. For UHPC, because of it's denser microstructure, the shrinkage caused by drying condition only occurs for about 20% of total shrinkage [14]. However, a remarkable rise in drying shrinkage was observed when high-volume of fly ash and GGBS was used for UHPC to replace Portland cement [73]. In addition, shrinkage increases with the increasing curing temperature after casting [73, 103]. This was because of the acceleration of hydration reactions, which results in higher chemical shrinkage and the nonuniform distribution of the hydration products. The former is considered as the main driving force for shrinkage until an internal rigid skeleton is formed [104-107]. It is reported that the shrinkage of UHPC could not be observed obviously until the curing temperature reached to

10

50°C during heat curing. While the curing temperature was close to 70°C, the value of shrinkage increased rapidly and reached to 450×10^{-6} ultimately as shown in Fig. 13 [108]. At the same time, the steam curing also increased the early autogenous shrinkage [109].
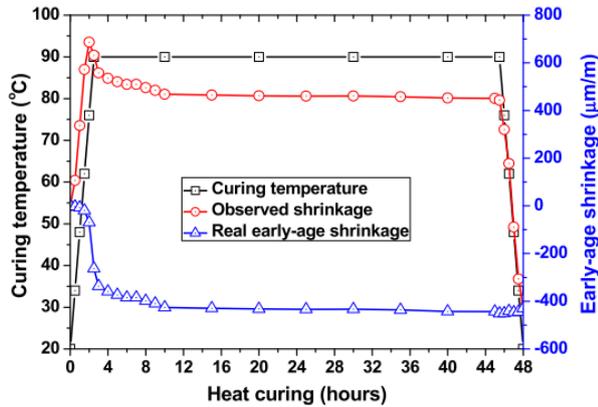
(a) Autogenous shrinkage of UHPC during heat curing period
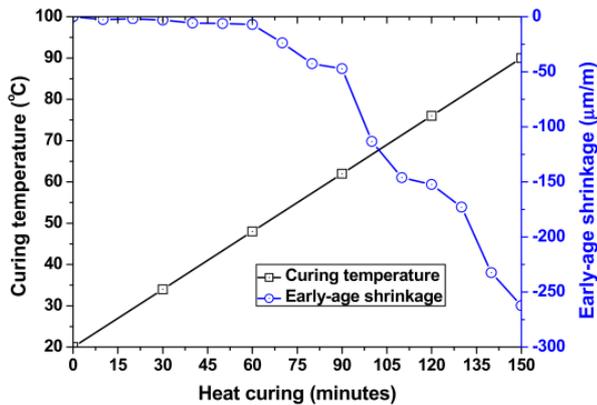
(b) Autogenous shrinkage of UHPC during temperature rise period

Fig. 13 Effect of heat curing on early age shrinkage of UHPC [108]

4.1.6 Fiber

As an essential component of fiber-reinforced concrete (FRC) for strengthening and toughening including UHPC, steel fiber can restrain shrinkage cracking. This is because high elastic modulus of steel fiber can reduce crack width and delay cracking propagation during the shrinkage developing process, including autogenous shrinkage. Wu and Shi [110] found that steel fiber volume had a significant effect in restraining shrinkage of UHPC, as shown in Fig. 14. It is found that the use of 2% steel fibers is the optimal dosage for reducing the autogenous shrinkage of UHPC. In addition, the evolution of autogenous shrinkage is influenced by the geometric characteristics of steel fiber, such as aspect ratio and fiber shape [110, 111]. With the increase of the aspect ratio of steel fiber, total shrinkage decreased [111].

In addition, the hooked fiber was more efficient in restraining shrinkage compared to the stra-ight and corrugated fibers, as shown in Fig. 13(b) [110]. The crimped and harex fibers were more effective in restraining autogenous shrinkage compared with melt extract and hooked fibers, owing to their superior anchorage characteristics [112]. Bouziadi found that polypropylene fiber is more effective than steel fiber in reduction of autogenous shrinkage of high performance concrete [111].
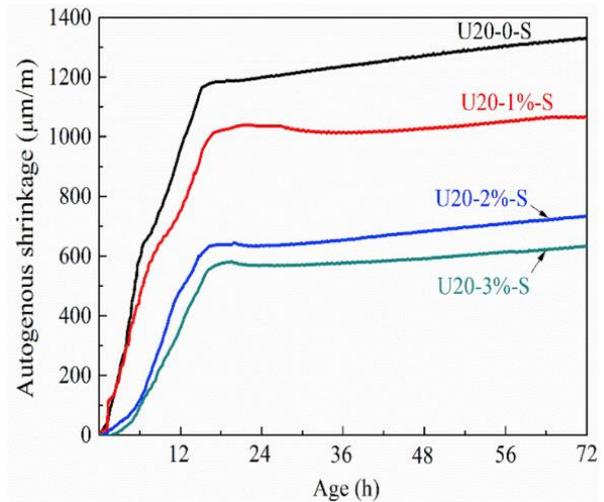
(a) Fiber content
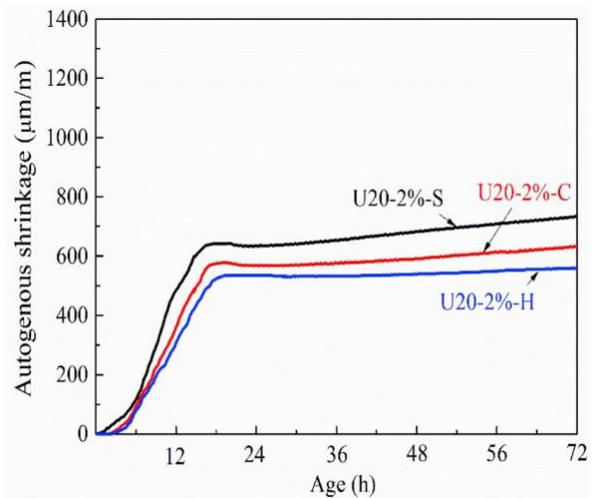
(b) Fiber type

Fig. 14 Effects of steel fiber on autogenous shrinkage of UHPC [110]

NOTE: S, C, and H represent straight, corrugated and hooked fibers, respectively.

4.2 Mitigation methods for shrinkage of UHPC

Typical UHPC mixtures are characterized by low w/b, high cement and SCMs content, and the incorporation of admixtures. A characteristic of UHPC's is its superior mechanical properties in the hardened state. However, at the moment of application, some difficulties arise, mainly because of its sensitivity to early-age cracking, which are associated

with self-desiccation and autogenous shrinkage. Cracking may lead to reduced strength, decreased durability, loss of prestress in prestressed structural elements, and structural integrity. Thus, it's important to understand and control autogenous shrinkage of UHPC.

The shrinkage, especially autogenous shrinkage, development of UHPC is related to hardening and hydration process. The capillary tension theory in general explicates the autogenous shrinkage using pore structure, relative humidity, self-stress, degree of hydration, and interface structure [71]. Over time, free water in the matrix gradually decreases due to progressive hydration of cement and SCMs, and chemical shrinkage occurs. This shrinkage appears as absolute volume change before initial setting, and creates capillary pores in the UHPC matrix. With ongoing hydration, the internal relative humidity reduces. Consequently, a large number of pores are formed in the hardened cement paste and the saturation of water in the pores declines. With the change in the saturation state of capillary pore from saturated to unsaturated, the inner concave surface of pore is subjected to an internal pressure. In order to make the concave surface in a state of equilibrium, the capillary tension increases by which autogenous shrinkage takes place. The capillary tension theory can well elaborate the accentuated influence of low water-to-cement ratio and SCMs in autogenous shrinkage of UHPC as they remarkably affect the pore structure, relative humidity, and self-stress, degree of hydration, and interface structure. Although some studies have addressed the effects of pore structure and relative humidity in particular on auto-genous shrinkage, some equations and model were established between the shrinkage stress with capillary pore diameter, internal relative humidity, and elastic modulus [8]. However, the roles of self-stress, degree of hydration, and interface structure are mostly discussed through influence of cement, SCMs, aggregates, and etc. and there is need for more research to consider the effects microstructure of matrix and interface. Based on previous discussion, different methods should be recommended to compensate for and/or reduce shrinkage of UHPC. Table 2 summarizes these different methods. Two or more methods are often combined to reduce autogenous shrinkage.

Table 2 Shrinkage compensating methods

Mechanism	Methods	Examples	Reference
Control hydration of binder materials	By adding SCMs to hinder early hydration or reduce hydration heat	Fly ash, metakaolin, and RHA, etc.	[82, 83, 113, 114]
	Reducing hydration temperature rise	Crushed ice	[62]
Reduce capillary tension	Restrain the drop of internal relative humidity (Internal curing)	Light-weight aggregate (LWA)	[65, 67]
		Super-absorbent polymer (SAP)	[14, 89, 102, 103, 115, 116, 117]
	Reduce surface tension of pore solution	Shrinkage reducing admixture (SRA)	[89, 111, 112]
Physical restrain	Increase tensile strength	Steel fiber and synthetic fiber	[110, 118]
	Hydration product with tendency to volume increase	Expansive agent (EA)	[90, 103, 119]

5. Conclusions and remarks

Based on the above literature review and discussions, the following conclusions can be drawn:

(1) The hydration of binders in UHPC is similar to that in OC. Silica fume and nanoparticles accelerate, whereas GGBS or fly ash retards the hydration of binder. When UHPC is cured under 90 °C, the average C–S–H chain length increases. If the curing temperature is raised to 250 °C, C–S–H will be dehydrated to form xonotlite.

(2) UHPC has a very low porosity, especially after heat curing. The microstructure of UHPC was greatly related to the addition of SCMs and curing conditions. Addition of silica fume or RHA could decrease the porosity of UHPC due to their filling and pozzolanic effects. However, the total porosity of the RHA modified sample was higher than that of the SF modified sample. GGBS had

little effect on the porosity of UHSC at early stages and increased the porosity of UHSC at later stages.

(3) The incorporation of nanomaterial as partial replacement for cement appears to be effective in improving the properties of UHPC. It can produce better dispersion and interaction of the reinforcement systems and achieve significantly higher mechanical strength and durability.

(4) The curing method has a great influence on microstructure of UHPC. High temperature curing is beneficial to the pozzolanic reactions between CH from the hydration of cement and supplementary binder materials, such as silica fume, which improves the microstructure. The autoclaved curing specimens exhibited dissolution processes around quartz grains, which produced a better cohesion between fillers and fine crystalline cement paste.

(5) UHPC with low water-to-binder ratios had high autogenous shrinkage. Aggregates can act as an internal restraint to reduce shrinkage, and also reduce the volume of cement paste, leading to lower chemical shrinkage. Shrinkage reducing agent (SRA) can decrease the surface tension of the capillary pore solution resulting in a reduction of the capillary tension, which lead to a significant reduction in the shrinkage of UHPC.

(6) Silica fume and GGBS were found to significantly increase the autogenous shrinkage due to refinement of the pore structure. However, incorporation of fly ash could decrease the shrinkage of concrete because the unhydrated binder material acted as aggregate to restrain shrinkage. Shrinkage increases with the increasing curing temperature. Fiber type and fiber shape also affect the shrinkage of UHPC.

(7) Different methods have been developed to compensate for and/or reduce early-age shrinkage of UHPC, such as internal curing, fiber, SRA, and EA. When the content is proper, some SCMs, such as fly ash, metakaoli, and RHA, also cloud reduce the autogenous shrinkage.

Reference

1. Richard, P., and Cheyrezy, M. (1995) "Composition of reactive powder concretes", Cem. Concr. Res., 25(7), pp. 1501-1511.

2. Shi, C.J.; Wu, Z.M.; Xiao, J.F.; Wang, D.H.; Huang, Z.Y.; and Fang, Z. (2015) "A review on ultra high performance concrete: Part I. Raw materials and mixture design", Constr. Build. Mater., 101, pp. 741-751.

3. Wang, D.H.; Shi, C.J.; Wu, Z.M.; Xiao, J.F.; Huang, Z.Y.; and Fang, Z. (2015) "A review on ultra high performance concrete: Part II. Hydration, microstructure and properties", Constr. Build. Mater., 96, pp. 368-377.

4. Wang, J.; Coombes, K.R.; Highsmith, W.E.; Keating, M.J.; and Abruzzo, L.V. (2004) "Differences in gene expression between B-cell chronic lymphocytic leukemia and normal B cells: a meta-analysis of three microarray studies", Bioinformatics, 20(17), pp. 3166-3178.

5. Pakravan, H.R.; Latifi, M.; and Jamshidi, M. (2017) "Hybrid short fiber reinforcement system in concrete: A review", Constr. Build. Mater., 142, pp. 280-294.

6. Tam, C.M.; Tam, V.W.Y.; and Ng, K.M. (2012) "Assessing drying shrinkage and water permeability of reactive powder concrete produced in Hong Kong", Constr. Build. Mater., 26(1), pp. 79-89.

7. Yazıcı, H.; Yardımcı, M.Y.; Aydın, S.; and Karabulut, A.Ş. (2009) "Mechanical properties of reactive powder concrete containing mineral admixtures under different curing regimes", Constr. Build. Mater., 23(3), pp. 1223-1231.

8. Liu, J.; Shi, C.; Ma, X.; Khayat, K.H.; Zhang, J.; and Wang, D. (2017) "An overview on the effect of internal curing on shrinkage of high performance cement-based materials", Constr. Build. Mater., 146, pp. 702-712.

9. Eppers, S. and Müller, C. (2008) "Autogenous shrinkage strain of Ultra-High-Performance Concrete (UHPC)" Paper presented at the Proceedings of the 2nd International Symposium on UHPC, Kassel, Germany, pp. 433-441.

10. Ichinomiya, T.; Hishiki, Y.; Ohno, T.; Morita, Y.; and Takada, K. (2005) "Experimental study on mechanical properties of ultra-high-strength concrete with low-autogenous-shrinkage", Special Publication, 228, pp. 1341-1352.

11. Lallemant-Gamboa, I.; Chanut, S.; Lombard, J.-P.; Chaignon, J.; and Thibaux, T. (2005) "Formulations, Characterizations and Applications of Ultra High-Performance Concrete", Special Publication, 228, pp. 1221-1236.

12. Fehling, E.; Leutbecher, T.; and Bunje, K. (2004) "Design relevant properties of hardened ultra high performance concrete", Paper presented at the Int. Symp. on Ultra High Performance Concrete., 1, pp. 327-338

13. Francisco, P.; Benboudjema, F.; Rougeau, P.; and Torrenti, J. M. (2009) "Ultra High Performance Concrete for Prestressed Elements. Interest of Creep Prediction", Designing and Building with UHPFRC, pp. 567-574.

14. Liu, J.; Farzadnia, N.; Shi, C.; and Ma, X. (2019) "Effects of superabsorbent polymer on shrinkage properties of ultra-high strength concrete under drying condition", Constr. Build. Mater., 215, pp. 799-811.

15. Wu, Z.M.; Shi, C.J.; and Khayat, K.H. (2016) "Influence of silica fume content on microstructure development and bond to steel fiber in ultra-high strength cement-based materials (UHSC)", Cem. Concr. Compos., 71, pp. 97-109.

16. Kadri, E.H. and Duval, R. (2009) "Hydration heat kinetics of concrete with silica fume", Constr. Build. Mater., 23(11), pp. 3388-3392.

17. Shi, C.; Wang, D.; Wu, L.; and Wu, Z. (2015) "The hydration and microstructure of ultra high-strength concrete with cement–silica fume–slag binder", Cem. Concr. Compos., 61, pp. 44-52.

18. Rong, Z.D.; Sun, W.; Xiao, H.J.; and Wang, W. (2014) "Effect of silica fume and fly ash on hydration and microstructure evolution of cement based composites at low water–binder ratios", Constr. Build. Mater., 51(2), pp. 446-450.

19. Langan, B.W.; Weng, K.; and Ward, M.A. (2002) "Effect of silica fume and fly ash on heat of hydration of Portland cement", Cem. Concr. Res., 32(7), pp. 1045-1051.

20. Wang, C.; Yang, C.H.; Liu, F.; Wan, C.J.; and Pu, X.C. (2012) "Preparation of Ultra-High Performance Concrete with common technology and materials", Cem. Concr.

Compos., 34(4), pp. 538-544.

21. WANG, C., PU, X.-C.; CHEN, K.; LIU, F.; WU, J.-H.; and PENG, X.-Q. (2008) "Measurement of Hydration Progress of Cement Paste Materials with Extreme-Low W/B", Journal of Materials Science & Engineering, 6, pp. 852-857.

22. Tang, M.-C. (2004) "High performance concrete—past, present and future", Paper presented at the Proceedings of the International Symposium on Ultra High Performance Concrete, Kassel, Germany., pp. 3-9

23. Shi, Y.X.; Matsui, I.; and Feng, N.Q. (2002) "Effect of compound mineral powders on workability and rheological property of HPC", Cem. Concr. Res., 32(1), pp. 71-78.

24. Zhu, W.Z. and Gibbs, J.C. (2005) "Use of different limestone and chalk powders in self-compacting concrete", Cem. Concr. Res., 35(8), pp. 1457-1462.

25. Svermova, L.; Sonebi, M.; and Bartos, P.J.M. (2003) "Influence of mix proportions on rheology of cement grouts containing limestone powder", Cem. Concr. Compos., 25(7), pp. 737-749.

26. Van Tuan, N.; Ye, G.; van Breugel, K.; and Copuroglu, O. (2011) "Hydration and microstructure of ultra high performance concrete incorporating rice husk ash", Cem. Concr. Res., 41(11), pp. 1104-1111.

27. Kang, S.-H.; Hong, S.-G.; and Moon, J. (2018) "The use of rice husk ash as reactive filler in ultra-high performance concrete", Cem. Concr. Res., 115,, pp. 389-400.

28. Wu, Z.M.; Shi, C.J.; Khayat, K.H.; and Wan, S. (2016) "Effects of different nanomaterials on hardening and performance of ultra-high strength concrete (UHSC)", Cem. Concr. Compos., 70, pp. 24-34.

29. Li, W.G.; Huang, Z.Y.; Zu, T.Y.; Shi, C.J.; Duan, W.H.; and Shah, S.P. (2016) "Influence of Nanolimestone on the Hydration, Mechanical Strength, and Autogenous Shrinkage of Ultrahigh-Performance Concrete", J. Mater. Civ. Eng., 28(1), pp. 04015068.

30. Sato, T. (2006) "Applications of nanotechnology for the sustainable

development of cement-based materials", University of Ottawa, ProQuest.

31. Ji, T. (2005) "Preliminary study on the water permeability and microstructure of concrete incorporating nano-SiO$_2$", Cement and Concrete Research, 35(10), pp. 1943-1947.

32. Meng, W. and Khayat, K.H. (2018) "Effect of graphite nanoplatelets and carbon nanofibers on rheology, hydration, shrinkage, mechanical properties, and microstructure of UHPC", Cem. Concr. Res., 105, pp. 64-71.

33. Muzenski, S.; Flores-Vivian, I.; and Sobolev, K. (2019) "Ultra-high strength cement-based composites designed with aluminum oxide nano-fibers", Constr. Build. Mater., 220, pp. 177-186.

34. Norhasri, M.S.M.; Hamidah, M.S.; and Fadzil, A.M. (2019) "Inclusion of nano metaclayed as additive in ultra high performance concrete (UHPC)", Constr. Build. Mater., 201, pp. 590-598.

35. Shen, P.; Lu, L.; He, Y.; Wang, F.; and Hu, S. (2019) "The effect of curing regimes on the mechanical properties, nano-mechanical properties and microstructure of ultra-high performance concrete", Cem. Concr. Res., 118, pp. 1-13.

36. Korpa, A.; Kowald, T.; and Trettin, R. (2009) "Phase development in normal and ultra high performance cementitious systems by quantitative X-ray analysis and thermoanalytical methods", Cem. Concr. Res., 39(2), pp. 69-76.

37. Kakali, G.; Tsivilis, S.; Aggeli, E.; and Bati, M. (2000) "Hydration products of C$_3$A, C$_3$S and Portland cement in the presence of CaCO$_3$", Cem. Concr. Res., 30(7), pp. 1073-1077.

38. Nehdi, M.; Mindess, S.; and Aïtcin, P.-C. (1996) "Optimization of high strength limestone filler cement mortars", Cem. Concr. Res., 26(6), pp. 883-893.

39. Rougeau, P. and Borys, B. (2004) "Ultra high performance concrete with ultrafine particles other than silica fume", Paper presented at the Ultra high performance concrete (UHPC). International symposium on ultra high performance concrete., 32, pp. 213-225

40. Yazıcı, H.; Yiğiter, H.; Karabulut, A.Ş.; and Baradan, B. (2008) "Utilization of fly ash and ground granulated blast furnace slag as an alternative silica source in reactive powder concrete", Fuel, 87(12), pp. 2401-2407.

41. Odler, I. (2003) "6–Hydration, Setting and Hardening of Portland Cement", Lea's Chemistry of Cement and Concrete (Fourth Edition), pp. 241-297.

42. Philippot, S.; Masse, S.; Zanni, H.; Nieto, P.; Maret, V.; and Cheyrezy, M. (1996) "29Si NMR study of hydration and pozzolanic reactions in reactive powder concrete (RPC)", Magn. Reson. Imaging, 14(7-8), pp. 891-893.

43. Zanni, H.; Cheyrezy, M.; Maret, V.; Philippot, S.; and Nieto, P. (1996) "Investigation of hydration and pozzolanic reaction in Reactive Powder Concrete (RPC) using 29Si NMR", Cem. Concr. Res., 26(1), pp. 93-100.

44. Cheyrezy, M.; Maret, V.; and Frouin, L. (1995) "Microstructural analysis of RPC (Reactive Powder Concrete)", Cem. Concr. Res., 25(7), pp. 1491-1500.

45. Feylessoufi, A.; Crespin, M.; Dion, P.; Bergaya, F.; Van Damme, H.; and Richard, P. (1997) "Controlled rate thermal treatment of reactive powder concretes", Advanced Cement Based Materials, 6(1), pp. 21-27.

46. Sorelli, L.; Constantinides, G.; Ulm, F.; and Toutlemonde, F. (2008) "The nano-mechanical signature of Ultra High Performance Concrete by statistical nano indentation techniques", Cem. Concr. Res., 38(12), pp. 1447-1456.

47. Bonneau, O.; Vernet, C.; Moranville, M.; and Aïtcin, P.-C. (2000) "Characterization of the granular packing and percolation threshold of reactive powder concrete", Cem. Concr. Res., 30(12), pp. 1861-1867.

48. Fehling, E.; Schmidt, M.; Teichmann, T.; Bunje, K.; Bornemann, R.; and Middendorf, B. (2005) "Entwicklung, Dauerhaftigkeit und Berechnung ultra-hochfester Betone (UHPC) [Development, durability and design of ultra-high strength concrete (UHPC)]", Research Report, University of Kassel, Structural Materials and Engineering, Kassel, Germany.

49. Long, G.; Xie, Y.; Wang, P.; and Jiang, Z. (2005) "PROPERTIES AND MICRO/MECROSTRU-

CTURE OF REACTIVE POWDER CONCRE-TE", Journal of the Chinese Ceramic Society, 33(4), pp. 456-461.

50. Alaee, F.J. (2002) "Retrofitting of concrete structures using high performance fibre reinforced cementitious composite (HPFRCC)", Doctoral dissertation, Cardiff University.

51. Yu, R.; Spiesz, P.; and Brouwers, H.J.H. (2015) "Development of an eco-friendly Ultra-High Performance Concrete (UHPC) with efficient cement and mineral admixtures uses", Cem. Concr. Compos., 55, pp. 383-394.

52. Mehta, P.K. and Monteiro, P.J.M. (2017) "Concrete Microstructure, properties and materials"., McGraw-Hill Publishing. Book

53. Gongqiu, H.Z.H. (2016) "Research on the shrinkage performance of ultra high performance concrete during heat curing", Materials Review(30 (2)), pp. 113-119.

54. Ollivier, J.; Maso, J.; and Bourdette, B. (1995) "Interfacial transition zone in concrete", Adv. Cem. Based Mater., 2(1), pp. 30-38.

55. Chan, Y.W. and Chu, S.H. (2004) "Effect of silica fume on steel fiber bond characteristics in reactive powder concrete", Cem. Concr. Res., 34(7), pp. 1167-1172.

56. Feylessoufi, A.; Villieras, F.; Michot, L.; De Donato, P.; Cases, J.; and Richard, P. (1996) "Water environment and nanostructural network in a reactive powder concrete", Cem. Concr. Compos., 18(1), pp. 23-29.

57. Lehmann, C.; Fontana, P.; and Müller, U. (2009) "Evolution of phases and micro structure in hydrothermally cured ultra-high performance concrete (UHPC)", *Nanotechnology in Construction 3* (pp. 287-293): Springer.

58. Shhmidt, M. and Fehling, E. (2007) "Grundlagen der Betontechnologie von Hochund Ultra Hochleistungsbeton und Anwendung von UHPC im Bruckenbau", Ultra High Performance Concrete–10 Years of Research and Development at the University of Kassal, Kassel, Germany, pp. 70-81.

59. Meng, W.; Samaranayake, V.; and Khayat, K.H. (2018) "Factorial Design and Optimization of Ultra-High-Performance Concrete with Lightweight Sand", ACI Mater. J., 115(1), pp.

129-138

60. Esping, O. (2007) "Early age properties of self-compacting concrete - Effects of fine aggregate and limestone filler", Doctoral dissertation, Sweden: Chalmers University of Technology.

61. Holt, E. (2005) "Contribution of mixture design to chemical and autogenous shrinkage of concrete at early ages", Cem. Concr. Res., 35(3), pp. 464-472.

62. Xie, T.; Fang, C.; Mohamad Ali M.S.; and Visintin, P. (2018) "Characterizations of autogenous and drying shrinkage of ultra-high performance concrete (UHPC): An experimental study", Cem. Concr. Compos., 91, pp. 156-173.

63. Cwirzen, A.; Penttala, V.; and Vornanen, C. (2008) "Reactive powder based concretes: Mechanical properties, durability and hybrid use with OPC", Cem. Concr. Res., 38(10), pp. 1217-1226.

64. Wang, X.; Wang, K.; Bektas, F.; and Taylor, P. (2012) "Drying shrinkage of ternary blend concrete in transportation structures", Journal of Sustainable Cement-Based Materials, 1(1-2), pp. 56-66.

65. Liu, J.; Shi, C.; Farzadnia, N.; and Ma, X. (2019) "Effects of pretreated fine lightweight aggregate on shrinkage and pore structure of ultra-high strength concrete", Constr. Build. Mater., 204, pp. 276-287.

66. Ma, X.; Liu, J.; and Shi, C. (2019) "A review on the use of LWA as an internal curing agent of high performance cement-based materials", Constr. Build. Mater., 218, pp. 385-393.

67. Meng, W. and Khayat, K. (2017) "Effects of saturated lightweight sand content on key characteristics of ultra-high-performance concrete", Cem. Concr. Res., 101, pp. 46-54.

68. Zou, D.; Li, K.; Li, W.; Li, H.; and Cao, T. (2018) "Effects of pore structure and water absorption on internal curing efficiency of porous aggregates", Constr. Build. Mater., 163, pp. 949-959.

69. Liu, J. and Shi, C. (2016) "Effects of fine-LWA as internal water curing agents on ultra-high strength cement-based materials (UHSC)", In C. Shi & D. Wang (Eds.), 1st International

Conference on UHPC Materials and Structures (Vol. 105, pp. 48-54). Bagneux: R I L E M Publications.

70. Tazawa, E.-I. (1999) "Autogenous shrinkage of concrete", CRC Press.

71. Wu, L.; Farzadnia, N.; Shi, C.; Zhang, Z.; and Wang, H. (2017) "Autogenous shrinkage of high performance concrete: A review", Constr. Build. Mater., 149, pp. 62-75.

72. Lim, S.N. and Wee, T.H. (2000) "Autogenous shrinkage of ground-granulated blast-furnace slag concrete", ACI Mater. J., 97(5), pp. 587-593.

73. Yalçınkaya, Ç. and Yazıcı, H. (2017) "Effects of ambient temperature and relative humidity on early-age shrinkage of UHPC with high-volume mineral admixtures", Constr. Build. Mater., 144, pp. 252-259.

74. Gleize, P.J.P.; Cyr, M.; and Escadeillas, G. (2007) "Effects of metakaolin on autogenous shrinkage of cement pastes", Cem. Concr. Compos., 29(2), pp. 80-87.

75. Brooks, J.J. and Johari, M.A.M. (2001) "Effect of metakaolin on creep and shrinkage of concrete", Cem. Concr. Compos., 23(6), pp. 495-502.

76. Kinuthia, J.M.; Wild, S.; Sabir, B.B.; and Bai, J. (2000) "Self-compensating autogenous shrinkage in Portland cement-metakaolin-fly ash pastes", Adv. Cem. Res., 12(1), pp. 35-43.

77. Staquet, S. and Espion, B. (2004) "Early age autogenous shrinkage of UHPC incorporating very fine fly ash or metakaolin in replacement of silica fume", Paper presented at the International Symposium on Ultra High Performance Concrete, Kessel, Germany., pp. 587-599

78. Termkhajornkit, P.; Nawa, T.; Nakai, M.; and Saito, T. (2005) "Effect of fly ash on autogenous shrinkage", Cem. Concr. Res., 35(3), pp. 473-482.

79. Arezoumandi, M. and Volz, J. S. (2013) "A comparative study of the mechanical properties, fracture behavior, creep, and shrinkage of high-volume fly ash concrete", Journal of Sustainable Cement-Based Materials, 2(3-4), pp. 173-185.

80. Sensale, G.R.D.; Ribeiro, A.B.; and Gonçalves, A. (2008) "Effects of RHA on autogenous shrinkage of Portland cement pastes", Cem. Concr. Compos., 30(10), pp. 892-897.

81. Habeeb, G.A. and Fayyadh, M.M. (2009) "Rice Husk Ash Concrete: the Effect of RHA Average Particle Size on Mechanical Properties and Drying Shrinkage", Australian Journal of Basic & Applied Sciences, 3(3), pp. 1616-1622.

82. Ye, G. and Nguyen, V.T. (2012) "Mitigation of Autogenous Shrinkage of Ultra-high Performance Concrete by Rice Husk", J. Chin. Ceram. Soc. (Eng), 40(2), pp. 212-216.

83. Van, V.T.A.; Rossler, C.; Bui, D.D.; and Ludwig, H.M. (2014) "Rice husk ash as both pozzolanic admixture and internal curing agent in ultra-high performance concrete", Cem. Concr. Compos., 53, pp. 270-278.

84. Rajabipour, F.; Sant, G.; and Weiss, J. (2008) "Interactions between shrinkage reducing admixtures (SRA) and cement paste's pore solution", Cem. Concr. Res., 38(5), pp. 606-615.

85. Rongbing, B. and Jian, S. (2005) "Synthesis and evaluation of shrinkage-reducing admixture for cementitious materials", Cem. Concr. Res., 35(3), pp. 445-448.

86. Zhang, W.; Hama, Y.; and Na, S. H. (2015) "Drying shrinkage and microstructure characteristics of mortar incorporating ground granulated blast furnace slag and shrinkage reducing admixture", Constr. Build. Mater., 93, pp. 267-277.

87. Yoo, D.Y.; Banthia, N.; and Yoon, Y.S. (2015) "Effectiveness of shrinkage-reducing admixture in reducing autogenous shrinkage stress of ultra-high-performance fiber-reinforced concrete", Cem. Concr. Compos., 64, pp. 27-36.

88. Kim, S.; Park, J.; Yoo, D.; and Yoon, Y. (2012) "Shrinkage Behavior of Ultra High Performance Concrete at the Manufacturing Stage", Proceedings of Hipermat, pp. 317-324.

89. Liu, J.; Farzadnia, N.; Shi, C.; and Ma, X. (2019) "Shrinkage and strength development of UHSC incorporating a hybrid system of SAP and SRA", Cem. Concr. Compos., 97, pp. 175-189.

90. Suzuki, M.; Maruyama, I.; and Sato, R. (2005) "Properties of Expansive-Ultra High-Strength

Concrete", Paper presented at the 7th International Symposium on Utilization of High-Strength/High-Performance Concrete, Edited by Henry G. Russell, America., pp. 1159-1174

91. Li, M.; Liu, J.P.; Tian, Q.A.; Wang, Y.J.; and Xu, W. (2017) "Efficacy of internal curing combined with expansive agent in mitigating shrinkage deformation of concrete under variable temperature condition", Constr. Build. Mater., 145, pp. 354-360.

92. Jensen, O.M. and Hansen, P.F. (2001) "Water-entrained cement-based materials I. Principles and theoretical background", Cem. Concr. Res., 31(4), pp. 647-654.

93. Zhu, Q.; Barney, C.W.; and Erk, K.A. (2014) "Effect of ionic crosslinking on the swelling and mechanical response of model superabsorbent polymer hydrogels for internally cured concrete", Mater. Struct., 48(7), pp. 2261-2276.

94. Schrofl, C.; Mechtcherine, V.; and Gorges, M. (2012) "Relation between the molecular structure and the efficiency of superabsorbent polymers (SAP) as concrete admixture to mitigate autogenous shrinkage", Cem. Concr. Res., 42(6), pp. 865-873.

95. Farzanian, K. and Ghahremaninezhad, A. (2018) "Desorption of superabsorbent hydrogels with varied chemical compositions in cementitious materials", Mater. Struct., 51(1), pp. 3.

96. Ma, X.W.; Liu, J.H.; Wu, Z.M.; and Shi, C.J. (2017) "Effects of SAP on the properties and pore structure of high performance cement-based materials", Constr. Build. Mater., 131, pp. 476-484.

97. Esteves, L.P. (2009) Internal curing in cement-based materials, Doctoral dissertation, Universidade de Aveiro (Portugal)

98. Lura, P.; Durand, F.; and Jensen, O.M. (2006) "Autogenous strain of cement pastes with superabsorbent polymers", International RILEM Conference on Volume Changes of Hardening Concrete: Testing and Mitigation, pp. 57-65.

99. Igarashi, S.-I. and Watanabe, A. (2006) "Experimental study on prevention of autogenous deformation by internal curing using super-absorbent polymer particles", Paper presented at the Volume changes of hardening concrete: testing and mitigation, Proceedings of the international RILEM conference, Denmark., pp. 77-86.

100. Zhutovsky, S. and Kovler, K. (2017) "Influence of water to cement ratio on the efficiency of internal curing of high-performance concrete", Constr. Build. Mater., 144, pp. 311-316.

101. Zhutovsky, S. and Kovler, K. (2013) "Hydration kinetics of high-performance cementitious systems under different curing conditions", Mater. Struct., 46(10), pp. 1599-1611.

102. Justs, J.; Wyrzykowski, M.; Bajare, D.; and Lura, P. (2015) "Internal curing by superabsorbent polymers in ultra-high performance concrete", Cem. Concr. Res., 76, pp. 82-90.

103. Soliman, A.M. and Nehdi, M.L. (2011) "Effect of drying conditions on autogenous shrinkage in ultra-high performance concrete at early-age", Mater. Struct., 44(5), pp. 879-899.

104. Acker, P. (2004) "Swelling, shrinkage and creep: a mechanical approach to cement hydration", Mater. Struct., 37(268), pp. 237-243.

105. Kamen, A.; Denarie, E.; Sadouki, H.; and Bruhwiler, E. (2008) "Thermo-mechanical response of UHPFRC at early age - Experimental study and numerical simulation", Cem. Concr. Res., 38(6), pp. 822-831.

106. Mounanga, P.; Khelidj, A.; Loukili, A.; and Baroghel-Bouny, W. (2004) "Predicting $Ca(OH)_2$ content and chemical shrinkage of hydrating cement pastes using analytical approach", Cem. Concr. Res., 34(2), pp. 255-265.

107. Jensen, O.M. and Hansen, P.F. (1999) "Influence of temperature on autogenous deformation and relative humidity change in hardening cement paste", Cem. Concr. Res., 29(4), pp. 567-575.

108. Li, W.G.; Huang, Z.Y.; Hu, G.Q.; Duan, W.H.; and Shah, S.P. (2017) "Early-age shrinkage development of ultra-high-performance concrete under heat curing treatment", Constr. Build. Mater., 131, pp. 767-774.

109. Graybeal, B.A. (2006) "Material property characterization of ultra-high performance concrete", No. FHWA-HRT-06-103., Office of Infrastructure Research and Development., Federal Highway Administration., United States.

110. Wu, Z.; Shi, C.; and Khayat, K.H. (2019) "Investigation of mechanical properties and shrinkage of ultra-high performance concrete: Influence of steel fiber content and shape", Composites Part B: Engineering, 174, 107021.

111. Bouziadi, F.; Boulekbache, B.; and Hamrat, M. (2016) "The effects of fibres on the shrinkage of high-strength concrete under various curing temperatures", Constr. Build. Mater., 114, pp. 40-48.

112. Mangat, P. and Azari, M. (1990) "Plastic shrinkage of steel fibre reinforced concrete", Mater. Struct., 23(3), pp. 186-195.

113. Staquet, S. and Espion, B. (2004) "Early age autogenous shrinkage of UHPC incorporating very fine fly ash or metakaolin in replacement of silica fume", Paper presented at the Int. Symp. on Ultra High Performance Concrete., pp. 587-599

114. Tuan, N.V.; Ye, G.; and van Breugel, K. (2010) "Internal Curing of Ultra High Performance Concrete by Using Rice Husk Ash", International Rilem Conference on Material Science (Matsci), Vol III, 77, pp. 265-274.

115. de Sensale; G.R. and Goncalves, A.F. (2014) "Effects of fine LWA and SAP as internal water curing agents", Int. J. Concr. Struct. & Mat., 8(3), pp. 229-238.

116. Kong, X.-M.; Zhang, Z.-L.; and Lu, Z.-C. (2014) "Effect of pre-soaked superabsorbent polymer on shrinkage of high-strength concrete", Mater. Struct., 48(9), pp. 2741-2758.

117. Wyrzykowski, M.; Ghourchian, S.; Sinthupinyo, S.; Chitvoranund, N.; Chintana, T.; and Lura, P. (2016) "Internal curing of high performance mortars with bottom ash", Cem. Concr. Compos., 71, pp. 1-9.

118. Meng, W. and Khayat, K.H. (2018). "Effect of Hybrid Fibers on Fresh Properties, Mechanical Properties, and Autogenous Shrinkage of Cost-Effective UHPC", J. Mater. Civ. Eng., 30(4), 04018030.

119. Park, C.-J. and Han, M.-C. (2015) "Mechanical Properties and Autogenous Shrinkage of Ultra High Performance Concrete Using Expansive Admixture and Shrinkage Reducing Agent depending on Curing Conditions", Journal of the Korea Academia-Industrial cooperation Society, 16(11), pp. 7910-7916.